Journal of Applied Electrochemistry **32**: 251–258, 2002.

Entropy change in lithium ion cells on charge and discharge

K. TAKANO*, Y. SAITO, K. KANARI, K. NOZAKI, K. KATO, A. NEGISHI and T. KATO
Energy Electronics Institute, National Institute of Advanced Industrial Science and Technology, AIST Tsukuba Central 2, 1-1-1, Umezono, Tsukuba-shi, Ibaraki 305-8568, Japan
*(*author for correspondence, fax: +81 298 61 5805, e-mail: k.takano@aist.go.jp)*

Received 23 February 2001; accepted in revised form 15 January 2002

Key words: conversion efficiency, entropy change, lithium-ion cell, phase change of $LiCoO_2$

Abstract

Open circuit voltage (OCV) was measured as a function of temperature and state of charge (SOC) for six kinds of lithium ion cells. The following cells were used: four kinds of commercial cell using a $LiCoO_2$ cathode and a graphite or hard carbon anode; a trial manufacture cell using a Li–Ni–Co complex oxide cathode and a graphite-coke hybrid carbon anode; and a trial manufacture cell using a $LiMn_2O_4$ cathode and a graphite anode. The entropy change in the cell reaction was determined by calculating the derivative of the OCV with temperature. Results were compared and discussed to determine the influence of the phase transition in the electrode materials due to cell reaction. It was clarified that the entropy change in cells using a $LiCoO_2$ cathode is negative except for the part of the SOC region where Li_xCoO_2 phase transition occurred. An endothermic reaction then occurs during discharge and an exothermic reaction during charge. In cells using $LiCoO_2$ cathodes, there was a fluctuation in the entropy change originating from the Li_xCoO_2 phase transition in the SOC range between 70% and 90%. This fluctuation was influenced by temperature and by additives or excess lithium in the cathode material. The entropy change in both cells using a Li–Ni–Co complex oxide cathode or a $LiMn_2O_4$ cathode was comparatively small.

1. Introduction

Lithium ion cells have been widely used for portable electronic devices, and have also been applied recently in commercial pure and hybrid electric vehicles in trials. Development of lithium ion cells with large capacity has been actively advanced with the aim of application to moving and stationary devices. It is very important to thermodynamically understand the thermal behaviour during discharging and charging to safely and efficiently utilize lithium ion cells, especially in the case of large capacity cells.

The entropy change in the electrochemical reaction is an important heat source in lithium ion cell during charge and discharge [1–3]. Thus, it is an important thermodynamic factor in cell thermal design and heat management.

The entropy change in the cell reaction can be obtained by measurement of the temperature dependency of the open circuit voltage (OCV) [4]. The entropy change can also be determined by calorimetric measurement during charge and discharge under reversible conditions in a cell [1]. Although there are some reports on the calorimetry of lithium ion cells, few reports on the entropy change have been obtained from the derivative of OCV with temperature [1, 3, 5]. A long time is needed for the OCV measurement; therefore only the entropy change data for a limited state of charge have been reported [3, 5]. This work did not investigate phase changes during charge and discharge in detail. In addition, temperature dependency of the entropy change remains to be clarified.

In this study, by measuring the OCV as functions of temperature in many states of charge during both intermittent discharge and charge, the entropy change ΔS in the cell reaction was examined for some representative lithium ion cells, compared among the cells and discussed with respect to phase change. The temperature dependency of ΔS was also examined.

2. Cell reaction and thermodynamic relations

The most common lithium-ion cell consists of $LiCoO_2$ as the cathode active material and graphite or hard carbon as the anode material. Cells using Ni oxides or Mn oxides for the cathode are being developed due to their lower cost. In the lithium ion cell, lithium ions are deintercalated from the cathode during charging and inserted into the anode. Reversely, during discharge, lithium ions are extracted from the anode and intercalated into the cathode. In a typical lithium-ion cell using $LiCoO_2$, the cell reactions of both positive and negative electrodes are as follows:

Positive electrode:

$$\mathrm{Li}_x\mathrm{CoO}_2 \underset{\text{discharge}}{\overset{\text{charge}}{\rightleftharpoons}} \mathrm{Li}_{x-\delta}\mathrm{CoO}_2 + \delta\mathrm{Li}^+ + \delta\mathrm{e}^- \quad (1)$$

Negative electrode:

$$\mathrm{Li}_y\mathrm{C}_m + \delta\mathrm{Li}^+ + \delta\mathrm{e}^- \underset{\text{discharge}}{\overset{\text{charge}}{\rightleftharpoons}} \mathrm{Li}_{y+\delta}\mathrm{C}_m \quad (2)$$

Whole cell reaction:

$$\mathrm{Li}_x\mathrm{CoO}_2 + \mathrm{Li}_y\mathrm{C}_m \underset{\text{discharge}}{\overset{\text{charge}}{\rightleftharpoons}} \mathrm{Li}_{x-\delta}\mathrm{CoO}_2 + \mathrm{Li}_{y+\delta}\mathrm{C}_m \quad (3)$$

In the case of an ideal reversible cell under the conditions of constant temperature and constant pressure, the enthalpy change, ΔH, and the entropy change, ΔS, in the cell reaction have the following relation with the Gibbs free energy change, ΔG [4]:

$$\Delta G = \Delta H - T\Delta S \quad (4)$$

The Gibbs free energy change, ΔG, can be converted into the work (electricity) in the ideal system, and it has the following relation with the electromotive force of the cell, E_{emf} [4]:

$$\Delta G = -nFE_{\mathrm{emf}} \quad (5)$$

From the thermodynamic relationship, the entropy change, ΔS, is given by the equation [4]:

$$\Delta S = -\frac{\partial \Delta G}{\partial T} \quad (6)$$

Thermodynamic parameters such as ΔG and ΔS are obtained from the measurement of the open circuit voltage, OCV, if the OCV can approximate the electromotive force E_{emf}.

$$\Delta G = -nF \times (\mathrm{OCV}) \quad (7)$$

$$\Delta S = nF\frac{\partial(\mathrm{OCV})}{\partial T} \quad (8)$$

3. Experimental details

3.1. *Sample*

The experiment was conducted on the six kinds of lithium ion cell shown in Table 1. Four samples, A, B, C and D, were commercial cells of which the cathode active materials was $LiCoO_2$. Two samples, E and F, were trial manufacture cells. The cathode active material of sample E was a Li–Ni–Co complex oxide, and that of sample F a $LiMn_2O_4$ spinel. Each commercial cell was the 18 650 size of 18 mm in diameter and 65 mm in length; and both trial manufacture cells were the 14 500 size of 14 mm in diameter and 50 mm in length. Three samples A, B and C, produced by different manufacturers, used graphite anodes. The sample A cathode contained Sn additive at about 2%. In sample D, a hard carbon (nongraphitizable carbon) was used for the anode; and the $LiCoO_2$ of the cathode was lithium rich [7]. The ratio of Ni/Co in the sample E cathode was 7:3, which was optimum for the capacity density [8]; and the anode consisted of a graphite and coke carbon hybrid. The $LiMn_2O_4$ of sample F was 2% rich in lithium.

3.2. *Method of measurement*

Cell samples were placed in an air-circulation type thermostatted chamber (Tabai Espec SU-220), the temperature of which was controlled by programming to the scan temperature of the cells. The cell temperature was measured by using a thermocouple attached to the surface of each cell and a recorder (Yokogawa HR3300). Cell voltage and current were measured by two digital voltmeters (Keithley 2000), synchronized with the cell temperature measurement. The state of charge (SOC) was adjusted using a multichannel charge–discharge battery tester (Kikusui 40W-08). After adjustment, the circuit was opened and only one digital voltmeter was connected during the OCV measurement. The data sampling interval was about 14 s.

The OCV of the lithium ion cells after discharge or charge did not become steady for hours. The OCV became steady more rapidly at the higher temperature because it seemed to be related to relaxation of the lithium distribution in the active materials. To minimize the influence on the OCV measurement with temperature scanning, the setting of the SOC and temperature scanning were conducted in the following sequence:

(i) Initial charge and discharge was done at a 0.2 C rate at 298 K. The temperature was then changed to 323 K, and the cell was fully charged at that temperature at 0.2 C constant current charge, followed by a constant voltage charge for a total period of 7 h.

Table 1. Lithium ion cells in the experiment

Sample	Cathode	Anode	Size	Comment
A	$LiCoMO_2$	Graphite	18650	A&T Battery
B	$LiCoO_2$	Graphite	18650	Panasonic
C	$LiCoO_2$	Graphite	18650	Sanyo
D	$LiCoO_2$	Hard Carbon	18650	Sony
E	$LiCo_{0.3}Ni_{0.7}O_2$	Hybrid Carbon	14500	Trial manufacture
F	$LiMn_2O_4$	Graphite	14500	Trial manufacture

Table 2. Initial normal discharge capacity, and accumulated discharge and charge capacities in the OCV measuring process

Sample	Q_0 /mA h	V_c/V	V_d/V	I/mA	Q_d/mA h	Q_c/mA h
A	1627.0	4.2	2.7	65	1598.3	1685.8
B	1356.0	4.2	2.7	54	1364.4	1450.5
C	1637.2	4.2	2.7	65	1592.4	1701.7
D	1284.7	4.2	2.7	52	1348.1	1354.0
E	611.4	4.1	2.7	24	539.1	631.7
F*	192.1	4.15	2.5	18	196.1	206.5

Q_0 normal discharge capacity in initial charge/discharge at 298 K.
V_c limited voltage in charging.
V_d cutoff voltage in discharging.
I charge and discharge current in SOC setting.
Q_d accumulated discharge capacity in OCV measuring process.
Q_c accumulated charge capacity in OCV measuring process.
*Q_0, Q_d and Q_c for sample F were measured at 303 K.

(ii) The cell was kept at the set SOC in the open circuit condition at 323 K for 20 h.
(iii) The chamber temperature was dropped to 283 K at 1 K min^{-1}, and then kept at a constant 283 K for 50 min.
(iv) The chamber temperature was increased to 323 K at 1 K min^{-1} and kept at 323 K constantly for 50 min.
(v) Return to (ii) after a 0.04 C constant current discharge for 1 h to set the next SOC; and repeat (ii)–(v) until the discharging voltage reached a certain cut-off voltage.

For measurement during the charging process, by carrying out periodic 0.04 C constant-current charge after finishing the measurements during the discharging process, a similar sequence of measurement was carried out. The constant voltage charge was carried out when the charging voltage reached the upper limit; and the constant voltage charge with a period of one hour was defined to be the fully charged condition. Discharge and charge currents for setting the SOC, the cutoff voltage for the discharge, and the voltage limit in the charge accompanying the initial discharge capacity are shown in Table 2.

4. Results and discussion

4.1. *State of charge*

Integrated values, Q_d (or Q_c), of the electrical quantity discharged (or charged) intermittently in the OCV measuring process are shown in Table 2 with the initial discharge capacity, Q_0, measured before the OCV measurement. The difference between Q_0 and Q_d is due mainly to two factors. One is the different measuring conditions such as the discharge rate and temperature. The other is thought to be the self-discharge because it becomes remarkable in about four weeks for the long-term OCV measurement at higher temperature. The degree of self-discharge can be evaluated from the difference between Q_c and Q_d.

As for the cell (sample F) using a $LiMn_2O_4$ spinel cathode, SOC adjustment and the OCV measurement at 323 K failed because cell degradation and self-discharge became too large. Therefore, the experiment on this sample was separately conducted at 303 K instead of at 323 K. The data for sample F in Table 2 are for 303 K. Self-discharge in the cell (sample E) using a Li–Ni–Co complex oxide cathode was also large following sample F. The difference between Q_c and Q_d for the samples A, B, and C using a graphite anode is 5%–7%, although the difference is small at about 0.5% in sample D using a hard carbon anode. According to a separately done capacity test, the difference between Q_0 and Q_d may be caused by the difference in the discharge rate in sample D.

Data such as OCV and its derivative are indicated as functions of SOC in the following. The SOC for 100% is defined as the state that is fully charged with the constant-voltage charge at a certain voltage which is shown in Table 2. The SOC was calculated from the accumulated electrical quantity with Q_d as the reference in the discharging process and Q_c as the reference in the charging process. Because the OCV changes with temperature, the fully charged condition is different at 298 K and 323 K. However, the difference is small below 1% in SOC, when it is estimated from the OCV sensitivities relative to both temperature and SOC as shown later. On the other hand, there is an uncertain difference in the SOC for 0% due to differences in the discharging rate and temperature.

4.2. *Variations of cell voltage and temperature*

Variations in cell voltage and temperatures in a series of measurements are shown in Figure 1 as an example. The typical relationships between the cell surface temperature and the OCV in the temperature scanning are shown in Figure 2. In many cases, the locus showed an approximately linear relation like (a) or (c) in Figure 2. Figures 1 and 2(b) show examples of SOC where a phase change from monoclinic to hexagonal in Li_xCoO_2 occurred due to temperature rise, as discussed later.

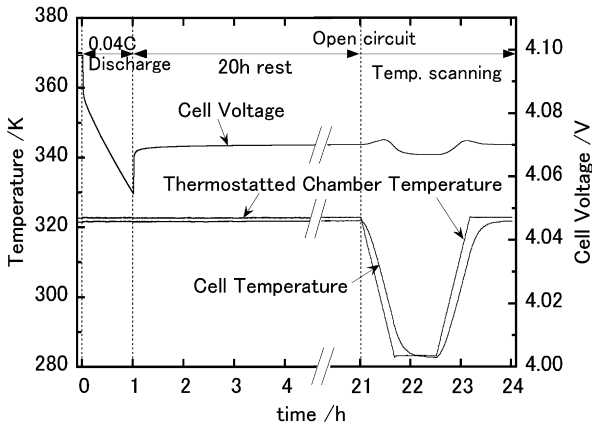

Fig. 1. An example of variations in cell voltage and temperatures in a series of OCV measurements at SOC = 82% for sample D during the discharge process.

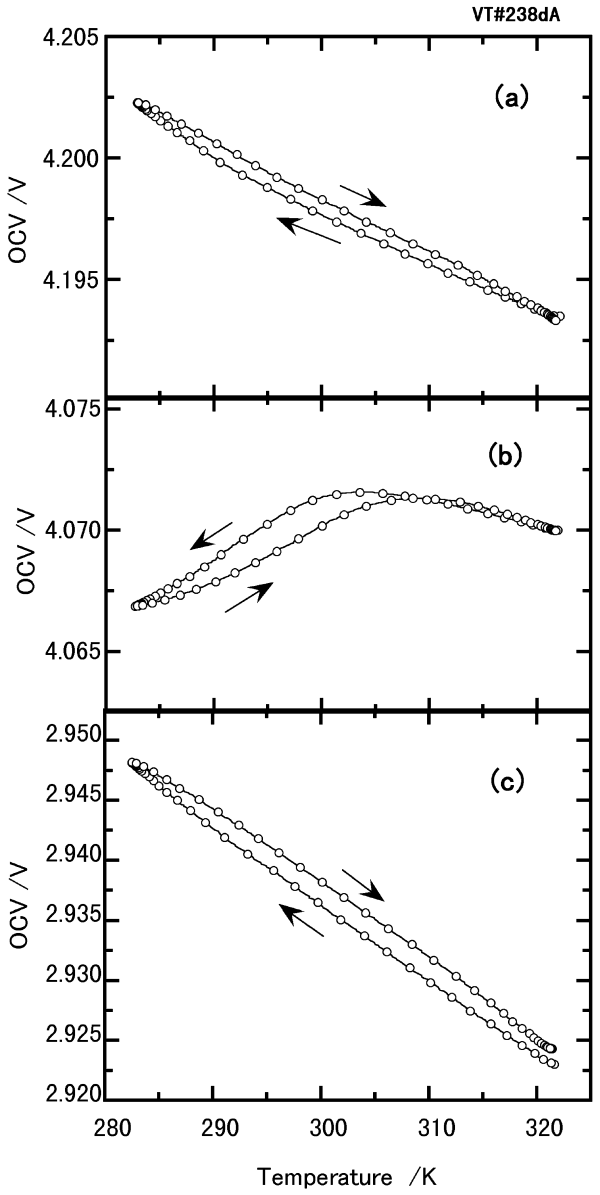

Fig. 2. Examples of typical changes in OCV against cell surface temperature in temperature scanning at SOC = 100% (a), SOC = 82% (b) and SOC = 0% (c) during the discharge process for sample D.

The curve of the OCV with a maximum as in Figure 2(b), is a special feature appearing in the phase-change region.

The locus of the OCV against temperature shows little difference between the fall and rise in temperature. Causes of the difference are considered to be: delayed temperature change inside the cell, relaxation of lithium distribution in the active materials, delayed phase change in the active materials etc. These factors cause errors in entropy change measurement.

The temperature distribution inside the cell was estimated to be about 1 K by thermal calculation for temperature scanning at 1 K min^{-1}; the delay in the temperature was also experimentally estimated to be about 5 K at maximum. The relaxation of lithium distribution in the active materials can be estimated from the difference in the OCV at steady state before and after a temperature scanning cycle. The difference between before and after was observed to be about 6 mV maximum at lower SOC. Self discharge also causes the difference in the OCV before and after the temperature scanning cycle and cannot be distinguished from the former. The difference in the locus is rather large in Figure 2(b) for the phase change region, and this supports the delay in the phase change.

It can be considered that most errors due to the above mentioned causes except for the delay in phase change may be compensated by averaging the derivatives of the OCV in temperature. Therefore, we used the mean value of the derivatives at a given temperature for both fall and rise in temperature. Errors estimated from the difference in the derivatives between the fall and rise were large in the phase change regions and the lower SOC; and were ± 0.12 mV K^{-1} at maximum and below ± 0.05 mV K^{-1} as root mean square values.

4.3. *Open circuit voltage (OCV)*

The OCVs of each cell measured in both discharge and charge as functions of SOC are shown in Figure 3. The OCV is the mean value at 303 K after 20 h on open circuit. At identical SOC, the OCV for the charging process is larger than that for discharging. In cells using $LiCoO_2$ cathodes, the difference in OCV between discharging and charging is different between a cell using a hard carbon anode and cells using graphite anodes. Samples A, B and C using graphite anodes showed similar difference in OCV between discharging and charging. Except for both SOC > 90% and SOC < 10%, the difference is as small as 10–45 mV. In sample D using a hard carbon anode, the difference for SOC over 50% is also as small as 30 mV or less. However, there is a large difference with a maximum of 180 mV at SOC between 0% and 50%; this seems to be due to hysteresis, which is a special feature of hard carbon, as reported by Xing et al. [8] and the authors [9]. In sample E, the difference in OCV between discharge and charge is comparatively large, 40–100 mV. This seems to be due to the graphite-coke hybrid carbon

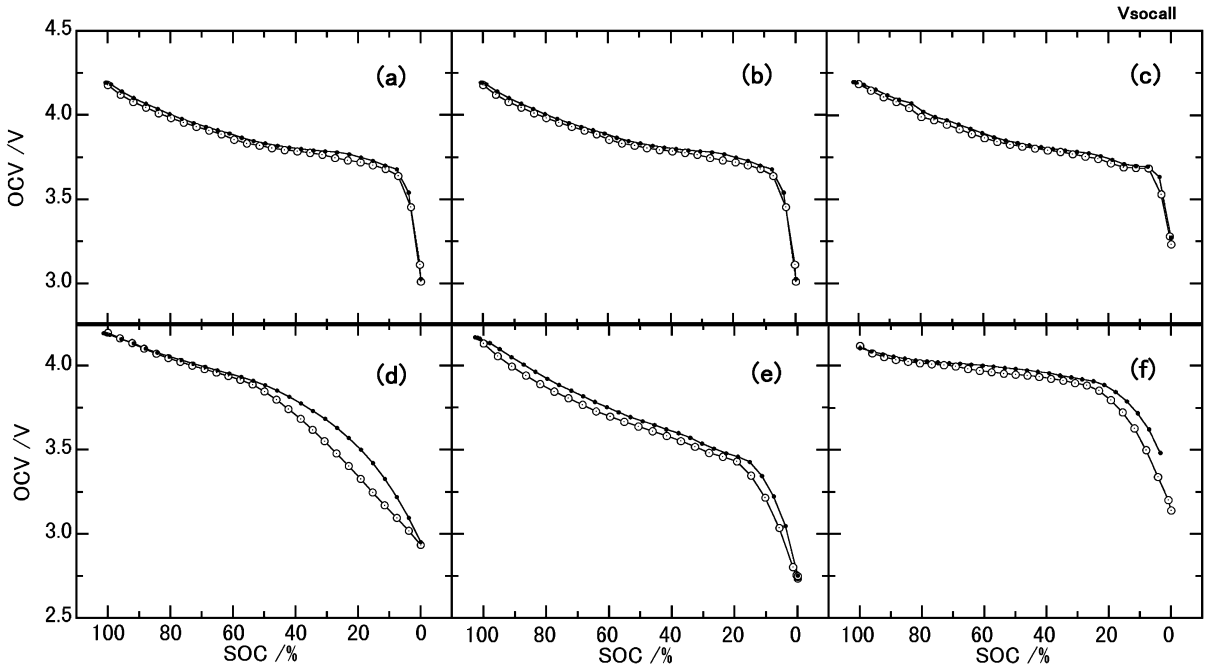

Fig. 3. OCV against SOC for the discharge process and charge process at 303 K. (a) Sample A, (b) sample B, (c) sample C, (d) sample D, (e) sample E and (f) sample F.

anode because coke carbon also shows hysteresis in the charge/discharge curve [10]. In sample F, using a $LiMn_2O_4$ cathode, the difference in OCV between discharge and charge increases with lower SOC, especially at 30% or less. The effect of the anode on the difference is considered to be similarly small in samples A, B and C because all use graphite anodes. Therefore, the difference in sample F may originate from the cathode.

4.4. *Derivative of OCV with temperature*

The derivative of OCV with temperature at 303 K at each state of charge in charge and discharge is shown in Figure 4. Derivatives of OCV for both processes change in approximately the same way. Especially, in sample D using a hard carbon anode, there is good coincidence over the whole SOC range, although hysteresis in the OCV appears in the SOC range between 0% and 50%.

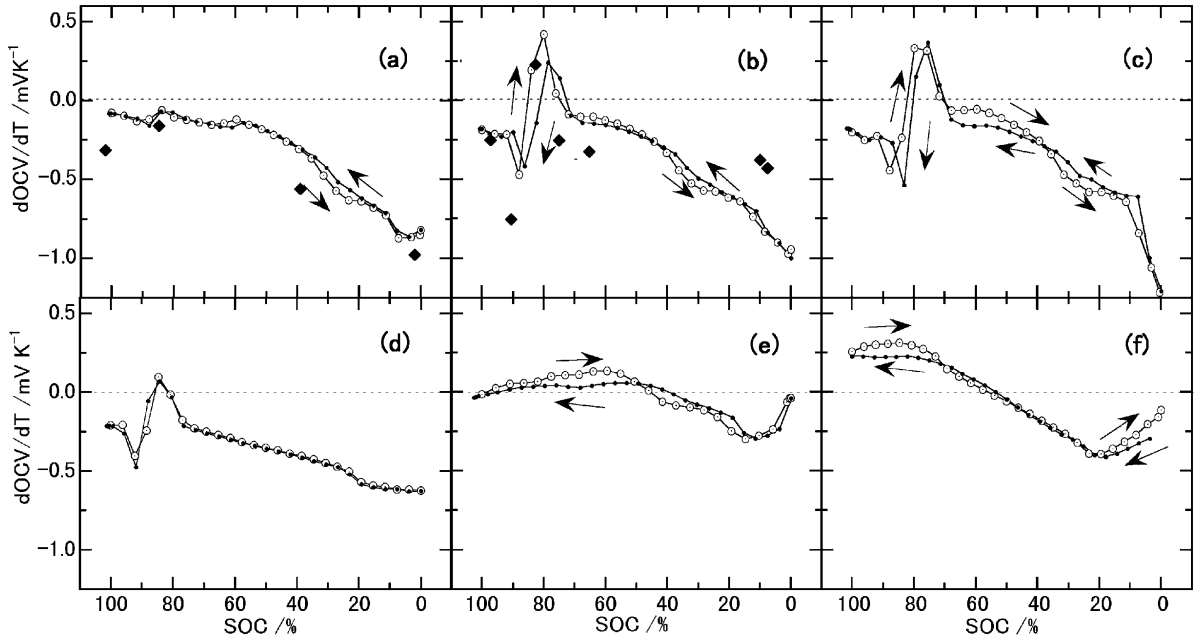

Fig. 4. Derivatives of OCV with temperature for discharging and charging at 303 K. (a) Sample A, (b) sample B, (c) sample C, (d) sample D, (e) sample E and (f) sample F. Key: (◆) data for the same battery manufacturers in [3]. Key: (⊙) discharge; (●) charge.

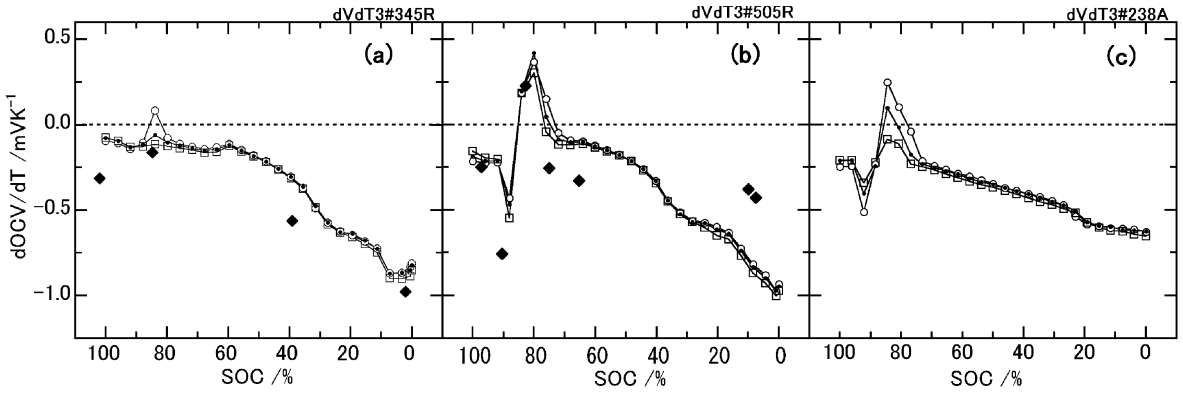

Fig. 5. Derivatives of OCV at different temperatures obtained during discharge process measurement. (a) Sample A, (b) sample B and (c) sample D. Key: (◆) data for the same battery manufacturers in [3]. Temperature: (○) 293, (●) 303 and (□) 313 K.

Noting the difference in both processes for samples A, B and C using graphite anodes, each inflection point in the curve of the derivative of OCV is shifted by 2%–5% in SOC between discharge and charge. Also, the difference increases in the SOC region between 20% and 30%. Because the shift in the SOC for the inflection point is smaller than the degree (5%–7%) of the difference between Q_d and Q_c, it is implied that the ambiguity of SOC due to self-discharge may be one reason for the shift.

A remarkable increase and decrease are seen in the derivative of OCV for the samples (A, B, C and D) using $LiCoO_2$ cathodes in the SOC between 70% and 90%. According to the composition analysis, the lithium content of Li_xCoO_2 in this SOC range is around 0.5 as the Li/Co ratio. It is well known that Li_xCoO_2 has monoclinic crystal structure near Li/Co = 0.5 and there is a change to a hexagonal structure when the Li/Co ratio deviates considerably from 0.5 [11, 12]. The change in the derivative of OCV, an entropy change, in this SOC range corresponds well to the results of calorimetry for the same samples [13]. The change in the derivative of OCV is speculated to be caused by the entropy change due to phase transition, hexagonal–monoclinic–hexagonal, in Li_xCoO_2 in the SOC range between 70% and 90%, as discussed earlier [1, 13].

Noting sample A using a graphite anode, there are other inflection-points near the SOC of 60%, 30%, and 10%, aside from those between 70% and 90%. They almost correspond respectively to 1/12, 1/24 and 1/48 at the Li/C ratio in graphite. These inflection points correspond well with calorimetry results [14]. Although it is well known that graphite intercalated by lithium assumes stage structures, changing stages near 1/12, 1/24 and 1/48 at Li/C ratios [15]. It is speculated that the inflections near the SOCs of 60%, 30% and 10% may be due to the stage structure change in the graphite [14]. Although some inflection points are not clear in samples B and C, the difference in the derivative between discharge and charge in samples A, B and C is clear in the SOC range between 20 and 30%. This suggests that the change in stage structure may be different between discharge and charge. In samples C, E and F there are other differences in the derivative of OCV between discharge and charge. The causes of these differences are not clear. However, the differences suggest that the crystal structure of the active materials may be different between the discharge and charge processes.

In all samples using a $LiCoO_2$ cathode, the derivative of OCV always has a negative value except for a part of the region where the phase transition in the cathode occurs. Both samples (E, F) using a Li–Ni–Co complex oxide cathode or a $LiMn_2O_4$ cathode have a special feature in which the derivative of OCV is positive or nearly zero in the half range of high SOC, and negative in the half range of low SOC.

Al Hallaj et al. measured the derivatives of OCV with temperature for two commercial lithium-ion cells [3]. One is a product of A&T Battery, and the other is a product of Panasonic. Both cells use graphite anodes and $LiCoO_2$ cathodes, and their capacities are different from the respective samples for the same manufacturers in this study. They showed an averaged derivative of OCV between 307 K and 323 K as a function of OCV. For comparison, the temperature derivative of OCV is also shown in Figures 4 and 5 by converting OCV to corresponding SOC. The data of Al Hallaj et al. do not agree well with our data. We can not determine the cause of the difference because of the different samples. However, Al Hallaj et al. carried out the OCV derivative measurement by increasing temperature from 307 K to 323 K in a staircase- or a ramp-like manner. In such case in our experiments, a large change was observed in OCV due to the relaxation of lithium distribution in the active materials as the temperature rose because the relaxation was insufficient at the lower temperature due to the lower rate. This fact could cause a large measurement error, so we made measurements only after sufficient relaxation at the higher temperature, as mentioned in Section 3.2. Also, our data agree well with calorimetric measurements during charge and discharge [13].

4.5. *Temperature dependency of the derivative of OCV*

For samples A, B and D using $LiCoO_2$ cathodes, derivatives of OCV with temperature at 293, 303 and 313 K obtained in discharge are shown in Figure 5. The derivatives hardly change with temperature in the range of 293 to 313 K except for the SOC range between 70% and 90%, where phase transition occurs in the cathode active material. In sample D, the derivative clearly changes with temperature in this SOC range, and its peak increases remarkably with reduced temperature. In sample A, the peak is difficult to recognize at 313 K, but it appears clearly at 293 K with reduced temperature. However, the change is not clear in sample B and sample C (not illustrated).

The reason why the temperature dependency of the derivative in the phase transition region is different among the samples of A, B (C) and D may be due to differences in precise composition of the cathode materials. The cathodes of samples B and C probably use the standard $LiCoO_2$ material, while the cathode of sample A contains Sn at about 2% and the $LiCoO_2$ of sample D is rich in lithium. According to Levasseur et al. [16], there is no phase transition to the monoclinic lithium-rich $Li_{1+x}CoO_2$, even if lithium is extracted at room temperature. According to Reimers et al. [17], the phase transition temperature to the monoclinic shifts down when a small amount of a different element such as Ni is added in $LiCoO_2$. From these facts, it is assumed that the transition temperature in samples A and D is lowered by the Sn additive or by excess lithium, resulting in a smaller transition heat even at 303 K. In fact, the lowering of the transition temperature in samples A and D was confirmed by differential scanning calorimetry [13].

In samples E and F the change due to the temperature in the derivative of OCV was small in the temperature range examined.

5. Conclusion

The open circuit voltage (OCV) in both discharge and charge was measured as a function of temperature for six kinds of lithium ion cells; four kinds of commercial cell using $LiCoO_2$ cathodes and graphite or hard carbon anodes, a trial manufacture cell using a Li–Ni–Co complex oxide cathode and a graphite-coke hybrid carbon anode, and a trial manufacture cell using a $LiMn_2O_4$ cathode and a graphite anode. The entropy change in the cell reaction was derived and discussed from these results with comparison among cells regarding influence of phase transition in the electrode materials. The following facts were clarified.

(i) The difference in OCV between the discharge process and charge process was small, at most 45 mV for cells consisting of $LiCoO_2$ and graphite electrodes. The OCV for the cells from three different manufacturers agreed fairly well.

(ii) The cell consisting of hard carbon and $LiCoO_2$ electrodes showed OCV change unlike the above-mentioned cells using a graphite anode. The OCV is noticeably different between discharge and charge in the SOC range below 50%, due to the voltage hysteresis of the hard carbon.

(iii) Change in OCV on discharge is larger in the cell using a Li–Ni–Co complex oxide cathode and a graphite-coke hybrid carbon anode than in the other cells, except for near the end of discharge. It is also smaller in the cell using a $LiMn_2O_4$ cathode.

(iv) The entropy change in the cells using a $LiCoO_2$ cathode is negative except for in a part of the Li_xCoO_2 phase transition region. This means that an endothermic reaction occurs during discharge and an exothermic reaction during charge. There is a fluctuation in the entropy change originating from the phase transition of Li_xCoO_2 in the SOC range between 70% and 90%. The fluctuation was influenced by temperature and by the additives and excess lithium in the cathode material.

(v) The entropy change in both cells using a Li–Ni–Co complex oxide cathode or a $LiMn_2O_4$ cathode is comparatively small. It has a positive value in the higher half of the SOC range, but it changes to a negative value in the lower half of the SOC range and approaches zero as an average over the whole SOC.

Acknowledgements

The trial manufacture cell with a Li–Ni–Co complex oxide cathode was offered by Sanyo Electric Co., Ltd in cooperative research with Lithium Battery Energy Storage Technology Research Association (LIBES) under a contact with New Energy and Industrial Technology Development Organization (NEDO). We thank Mr. N. Terada of LIBES, Dr I. Yonezu of Sanyo Electric Co., Ltd, and all parsons concerned.

References

1. Y. Saito, K. Takano, K. Kanari and T. Masuda, *Bull. Electrotechnical Lab.* **60** (1996) 771.
2. J-S. Hong, H. Maleki, S.A. Hallaj, L. Redey and J.R. Selman, *J. Electrochem. Soc.* **145** (1998) 1489.
3. S. Al Hallaj, L.J. Prakash and J.R. Selman, *J. Power Sources* **87** (2000) 186.
4. A.J. Bard and L.R. Faulkner, 'Electrochemical Methods, Fundamentals and Applications', (J. Wiley & Sons, New York 1980), pp. 48–49.
5. R. Yazami, *in* G. Pistoia (Ed.), 'Lithium Batteries', (Elsevier, Amsteram, 1994) pp. 49–92.
6. K. Ozawa, *Solid State Ionics* **69** (1994) 212.
7. I. Yonezu, T. Maeda, Y. Chikano, K. Ohkita, H. Kurokawa, T. Nohma and K. Nishio, 'Development of 250 Wh Class Lithium Secondary batteries with a Graphite-Coke Hybrid Carbon Negative Electrode and a $LiNi_{1-x}Co_xO_2$ Positive Electrode', The EVS-15 CD-ROM Proceedings of the 15th international electric vehicle symposium, Brussels, Belgium, 1–3 Oct. (1998).

8. W. Xing, J.S. Xue and J.R. Dahn, *J. Electrochem. Soc.* **143** (1996) 3046.
9. Y. Saito, K. Takano, K. Kanari and K. Nozaki, 'Voltage Hysteresis and Heat Generation Behavior in Lithium-ion Batteries', the Proceedings of Materials Research Society Symposium 496, Materials for Electrochemical Energy Storage and Conversion II – Batteries, Capacitors and Fuel Cells, Boston, MA, 1–5 Dec. (1997), pp. 551–556.
10. J.R. Dahn, R. Fong and M.J. Spoon, *Phys. Rev. B* **42** (1990) 6424.
11. J.N. Reimers and J.R. Dahn, *J. Electrochem. Soc.* **139** (1992) 2091.
12. T. Ohzuku and A. Ueda, *J. Electrochem. Soc.* **141** (1994) 2972.
13. Y. Saito, K. Takano, K. Kanari, A. Negishi, K. Nozaki and K. Kato, *J. Power Sources* **97–98** (2001) 688.
14. Y. Saito, K. Takano, K. Kanari and A. Negishi, 'Thermal Measurements of Rechargeable Lithium Battery (7), Thermal Behaviors of the Batteries with Graphite', Proceedings of the 40th Battery Symposium in Japan, Kyoto, Japan, 14–16 Nov. (1999), pp. 379–380.
15. J.R. Dahn, *Phys. Rev. B* **44** (1991) 9170.
16. S. Levasseur, M. Menetrier, E. Suard and C. Delmas, *Solid State Ionics* **128** (2000) 11.
17. J.N. Reimers, J.R. Dahn and U. von Sacken, *J. Electrochem. Soc.* **140** (1993) 2752.